



## Characterization of Silver and Magnetite Nanoparticles Synthesized with *Cleome Heratensis*

**Nikhil Parsotambhai Ramoliya**

Research Scholar, Surendrangar University, Wadhwan City, Gujarat

In recent decades, development of green and reliable processes for synthesis of metallic nanoparticles is inevitable because of their important applications in all fields of science, especially in nanotechnology and industry. Biological systems have received great attentions from scientist due to low cost, green nature and simple process for the synthesis of metallic NPs. In this research, metal nanoparticles, Ag and Fe<sub>3</sub>O<sub>4</sub> NPs were synthesized through an ecofriendly and cost-effective approach using aqueous extract of *Cleome heratensis* (*C. heratensis*). The influence of effective parameters including pH, interaction time, temperature, plant extract concentration, and Ag concentration were thoroughly investigated base on surface plasmon resonance (SPR) for Ag NPs at  $\lambda_{\max} \sim 470$  nm. The bio-synthesized NPs were characterized by FTIR, UV-Vis, XRD, TEM and VSM analyses. The TEM images showed the size of silver and magnetite nanoparticles as 12.27 and 14.12 nm, respectively, with a homogeneous distribution and nearly spherical in shape.

**Keywords:** *C. heratensis*, Capparaceae, Biosynthesis, Silver nanoparticles, Magnetite nanoparticles

### INTRODUCTION

Nanomaterials are found to be attractive and promising inevitable tools in modern science due to their unique properties compared to the corresponding bulk materials, such as catalytic, optical, conductivity, mechanical, *etc.* [1-3]. These properties are based on their size, shape, morphology, and distribution arising from quantum confinement of electrons in



nanoparticles [4]. Also, they have a high surface to volume ratio (aspect ratio) that is inversely proportional to their size, providing a huge surface for various purposes [2]. Among several NPs, silver and iron oxide metal NPs have received lots of attention due to their unique physical and chemical properties in electro analytical, electrochemical, and bio-electrochemical applications [3,5]. Ag NPs have electrical, thermal, optical and biological (antimicrobial and antifungal, anti-cancer, larvicidal, and anti-parasitic agent), catalytic and surface-enhanced Raman scattering properties [6]. Considering the properties of iron oxide metal NPs, they are increasingly used in various fields of application including food industries [7], textile industries [8] (Ag impregnated fabrics), biomedical (*e.g.*, in skin ointments and creams for inhibition of infection and wound) [9], consumer products, drug delivery [10], optical sensors [11], cosmetics [3], in diagnostics, health care [12], *etc.* Additionally, superparamagnetic Fe<sub>3</sub>O<sub>4</sub> NPs have attracted a great deal of attention due to their particular properties such as small size, high magnetism behavior, biocompatible, biodegradable and low toxicity [13], which could be used as magnetic resonance imaging (MRI) in sensors and biosensor [14], as catalyst and solid support [15], as high-density magnetic recording media [16], for targeted drug delivery [17], and as substrates in cancer treatment methods [18]. There are various approaches for the synthesis of Ag and Fe<sub>3</sub>O<sub>4</sub> NPs including physical and chemical methods such as micro-emulsion [19], microwave assisted process [20], polyol process [21], and reduction through chemical, radiation, electrochemical and photochemical methods [22] for Ag NPs and sol-gel method [23], solid state synthesis [24], and flame spray synthesis [25] for Fe<sub>3</sub>O<sub>4</sub> NPs. However, these methods usually involve disadvantages such as high cost, toxic, tedious work-up and non-environmentally friendly performance with high consumption of time and energy [26]. So, due to their widespread applications in all of the field science, finding safer, green, low cost and eco-friendly protocols for synthesis of NPs is in demand. Recently, extensive efforts have been made to use biological systems (plant and fruit extract, bio-organism, enzymes, *etc.*) as a clean and ecofriendly approach for biosynthesis of NPs overcoming most of the disadvantages regarding to the previously reported methods [27,28]. Among biological approaches, plant extracts are the most popular method in synthesizing NPs due to the low consumption of time and energy (it could be readily scaled up for large scale NPs synthesis) as well as green



chemistry speculations. It was shown that plant extract as a renewable and green resource in the synthesis of NPs, not only cap and stabilize the particles, but also act as a reducing agent transferring the metal ions to metal nanoparticles [29]. Although the nature of the reducing agents involved is not well understood, efficient performance of the plant extracts is mostly attributed to the, presence of some bioactive molecules such as proteins, carbonyl groups, terpenoids, phenolics, amines, flavonones, amides, pigments, and alkaloids [30-32] acting as stabilizing agents [29]. There are many reports to date on plant extract- mediated biosynthesis of Ag NPs including: *Ficus benghalensis* [33], *Aloevera* [34], *Talinum triangulare* [35], *Abutilon indicum* [36], *Azadirachta indica* [37], *Mussaenda glabrata* [38], basil [39], *Shikakai* and *Reetha* [40], *Tamarind fruit* [41], *Ipomoea asarifolia* (*Convolvulaceae*) [42], *Syzygium aromaticum* [43], *Radix Puerariae* [44], *Vaccinium macrocarpon* [45], and *alliandrahaematocephala* [46].

Despite extensive studies on the preparation of nanoparticles using various plants, given the importance and widespread use of metal nanoparticles in various sciences, providing a reliable, green, more accessible, easy handling alternative method with high efficiency appear to be necessary. *Cleome heratensis* (*C. heratensis*) flower belongs to the family *Cleomaceae* [47], which is an annual herbaceous plant growing in warm areas during summer and autumn. The germinating, flowering and fruiting stage of this plant occur in May, September and October, respectively [48]. It has medicinal properties such as headache, earache, skin diseases and rheumatism in traditional medicine [49,50]. Herein, we have reported the biosynthesis of Ag and Fe<sub>3</sub>O<sub>4</sub> NPs using the *Cleome heratensis*. extract as a reducing and capping agent through a fast, green and simple protocol. In the following, the reaction parameters including pH, temperature, interaction time, AgNO<sub>3</sub> and plant extract concentration are investigated in order to achieve the highest possible efficiency for the NPs.

## EXPERIMENTAL

### Materials and Methods

*C. heratensis* was collected in late September and October 2014 from South Khorasan, Birjand, Iran. All the chemicals were of analytical reagent grade purchased from Sigma Aldrich and used as received without further purification.



Acetic acid, sodium hydroxide and silver nitrate were purchased from Sigma and Merck companies.  $\text{FeCl}_3 \cdot 6\text{H}_2\text{O}$  and  $\text{FeSO}_4 \cdot 4\text{H}_2\text{O}$  were purchased from Riedel-de Haen (Seelze, Germany).

### Preparation of Plant Extract

Aerial parts (Fig. 1) of *C. heratensis* were rinsed with deionized water, air-dried at room temperature, then finely meshed and grinded with mortar and pestle. Then, 5 g of the plant powder was added to 100 ml deionized water. The mixture was then mechanically stirred and boiled for 5 min, then cooled to room temperature and finally filtered through Whatman No. 1 filter paper. The filtrate is used immediately for the biosynthesis of Ag and  $\text{Fe}_3\text{O}_4$  NPs.

### Synthesis of Silver Nanoparticles

25 ml of aqueous solution of  $\text{AgNO}_3$  (0.025 M) was prepared and added dropwise into 25 ml of the *C. heratensis* extract. The resultant mixture was mechanically stirred at 100 °C for 6 h. Reduction of silver nitrate to silver NPs was certified by the color change from light to dark brown. The silver nanoparticles were obtained by centrifugation of the mixture (4600 rpm) for 30 min followed by re-dispersion in deionized water in order to elimination of any uncoordinated biological molecules [51]. The centrifugation and re-dispersion in deionized water were repeated for three times.





## Synthesis of Magnetite Nanoparticles

The extract of the aerial parts of *C. heratensis* was also served for the bio-synthesis of magnetite NPs ( $\text{Fe}_3\text{O}_4$ ). The bio-synthesis of  $\text{Fe}_3\text{O}_4$  NPs using *C. heratensis* were performed according to a previously reported procedure [52].  $\text{FeCl}_2 \cdot 4\text{H}_2\text{O}$  (0.265 g) and  $\text{FeCl}_3 \cdot 6\text{H}_2\text{O}$  (0.555 g) were dissolved in 50 mL of deionized water and heated at 100 °C under vigorous stirring and atmospheric pressure for 10 min. Then, 5 ml of the aqueous solution of *C. heratensis* extract was added to the mixture. Color of the mixture was immediately changed to reddish brown. The mixture was stirred for further 5 min, then 12 ml of sodium hydroxide aqueous solution was added to the mixture with rate of 3 mL/min in order to formation of uniform nanoparticles [44]. The magnetite NPs were collected by an external magnetic field and rinsed with deionized water (3 x 20 ml) followed by centrifugation to remove heavy biomaterials.

## Optimization of Reaction Parameters

Different parameters involved in the bio-synthesis of NPs including pH, time, temperature concentration of silver nitrate and concentration of extract were thoroughly investigated in order to achieve the highest efficiency for the bio-synthesis of NPs. These parameters were optimized for Ag NPs that could be generalize for the bio-synthesis of  $\text{Fe}_3\text{O}_4$  NPs.

**Effect of extract concentration.** Different concentrations (1/10, 1/20, 1/30, 1/40, 1/50) of the aqueous extract of *C. heratensis* were prepared by boiling 1 g of aerial parts of the plant in 10, 20, 30, 40, 50 ml of deionized water for 5 min. The biosynthesis of Ag NPs was conducted at various extract concentrations while temperature,  $\text{AgNO}_3$  concentration, and pH were kept constant at 100 °C, 0.025 M and 9, respectively, at 1:1 mixing ratio for 4 h.

**Effect of  $\text{AgNO}_3$  concentration.** Different concentrations of  $\text{AgNO}_3$  aqueous solution (0.1, 0.05, 0.025, 0.0125, 0.062 M) were added to aqueous extract of *C. heratensis* (1/20) while other reaction conditions kept constant.

**Effect of interaction time.** To investigate the effect of interaction time on the biosynthesis of Ag NPs, the aqueous extract of *C. heratensis* (1/20 concentration) was interacted with 0.025 M  $\text{AgNO}_3$  in 1:1 mixing ratio for different time intervals (ranging



from 30-240 min).

**Effect of interaction temperature.** Influence of temperature on the bio-synthesis of Ag NPs was studied by measuring the absorption spectra of the solution at the different temperature (r.t., 60, 70, 80, 90, 100, 110, 120 °C) for 4 h.

**Effect of pH.** To investigate the pH effect on the biosynthesis of Ag NPs, the pH of aqueous solution of AgNO<sub>3</sub> was varied as 4, 5, 7, 8, 9 and 10 using dilute acetic acid and sodium hydroxide solutions. The aqueous extract of *C. heratensis* (1/20 concentration) was treated with 0.025 M AgNO<sub>3</sub> solutions at different pH values for 4 h.

### Characterization of Nanoparticles

FTIR spectra of the extract and as-prepared nanoparticles were recorded by Fourier transform infrared spectroscopy Lambda 45, Perkinelmer, USA. The FTIR spectrum ranged from 4000 to 400 cm<sup>-1</sup> at a resolution of 4 cm<sup>-1</sup> by making a KBr pellet with NPs. The reduction of Ag<sup>+</sup> ions as well as investigations on reaction parameters were monitored by recording the UV-Vis spectra between 200-800 nm wavelengths on a Shimadzu UV-Win X-ma 2000 spectrophotometer. To determine the crystal structure of the bio-synthesized NPs, their X-ray diffraction pattern were obtained on an Analytical X-ray diffractometer instrument with X'Pert high score plus software operated at a voltage 40 kV and a current 30 mA with Cu Ka radiation with X of 1.5406 Å and nickel monochromator. The scanning was performed in the region of 2θ from 10° to 81°. The size, shape and morphology of the nanoparticles were observed using a transmission electron microscopy (TEM) JEOL 2100, Japan instrument at an accelerating voltage of 100 kV. The magnetization hysteresis loop was applied for manifestation of the magnetic behavior of bio-synthesis Fe<sub>3</sub>O<sub>4</sub> NPs using vibration sample magnetometer, VSM; Lake Shore Model 7400, Japan instrument under magnetic fields up to 10 kOe at room temperature.

### RESULTS AND DISCUSSION

UV-Vis spectroscopy is a valuable technique for the analysis of metal nanoparticles [37]. The NPs showed the absorption band at X<sub>max</sub>~ 470 nm due to the surface Plasmon resonance (SPR) of metal electrons, which provide information about the size and shape of the NPs [53,54]. Furthermore, color change of the solution from pink to black after addition of



AgNO<sub>3</sub>, arising from Ag-SPR band, was another evidence for the bio-synthesis of Ag NPs (Fig. 2B) [28]. Figure 2A shows recorded UV-Vis spectra for aerial parts of *C. heratensis* extract and bio-synthesized silver NPs. The peak appeared at ~470 nm demonstrated SPR band for Ag NPs, which is in agreement with the reported spherical Ag NPs absorption band [55] and subsequently confirms the preparation of the NPs. Electronic spectra for the extract showed an absorption band at ~305 nm (Fig. 2A).

### Optimization Study

It was proved that the position of SPR band are influenced by the size, shape and morphology of the prepared NPs [56], which is directly proportional to the reaction parameters. So, finding optimum conditions is a key step for biosynthesis of metallic NPs. To find the optimum conditions for the preparation of NPs, experiments were performed over the bio-synthesis of Ag NPs according to the SPR absorption band of Ag NPs at ~470 nm. The obtained results could be developed for the biosynthesis of Fe<sub>3</sub>O<sub>4</sub> NPs using *C. heratensis* plant extract.

**Effect of interaction time.** To investigate the effect of interaction time on the biosynthesis of Ag NPs, aqueous extract of the *C. heratensis* (1/20 concentration) was treated with AgNO<sub>3</sub> (0.025 M) in 1:1 mixing ratio, then the electronic spectra were recorded at different time intervals. As shown in Fig. 3a, with increase of time from 30 min to 240 min, a red shift was observed in X<sub>max</sub> from 440 to 470 nm. The increase of absorbance as a function of time implies the progress of the Ag<sup>+</sup> reduction to form Ag NPs. This progress was also verified by the images of the solution at different time intervals, where the color of the solution changed from pink to black (Fig. 3b). Also, a red shift was observed for the SPR band from 430 to 470 nm, confirmed the color change and preparation of Ag NPs. This red shift is due to the effect of capping agents with increasing particle size obtained by the slow diffusion by reducing agents [57]. The absorption band at X ~ 470 nm belonging to SPR of Ag NPs increased as a function of time in 240 min time interval. The results suggest that reduction of silver ions efficiently takes place for 240 min. No change was detected in the SPR band intensity after more time of the reaction, indicating the completion of the reduction of silver ions (not shown in the figure).



VIDHYAYANA

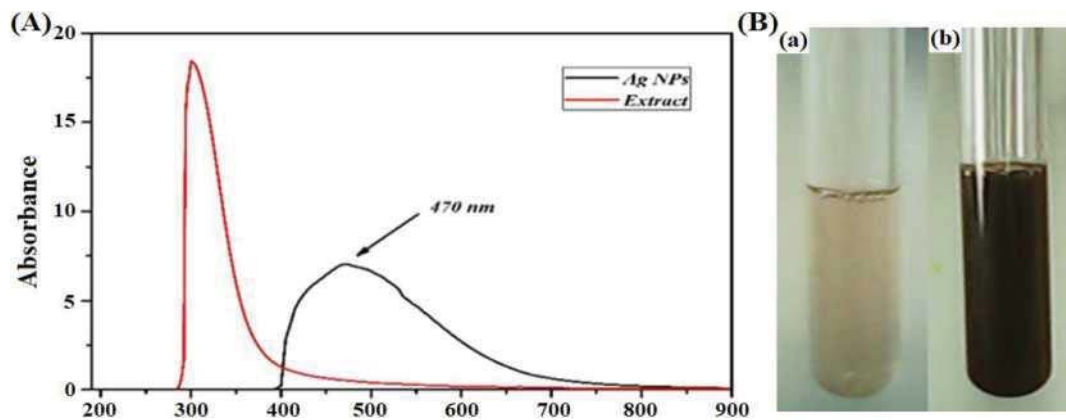


**Fig. 2.** (A) UV-Vis spectra of the bio-synthesized silver NPs and *C. heratensis* extract. (B) Color changes of the extract (a) before and (b) after synthesis of NPs (after addition of  $\text{AgNO}_3$ ).

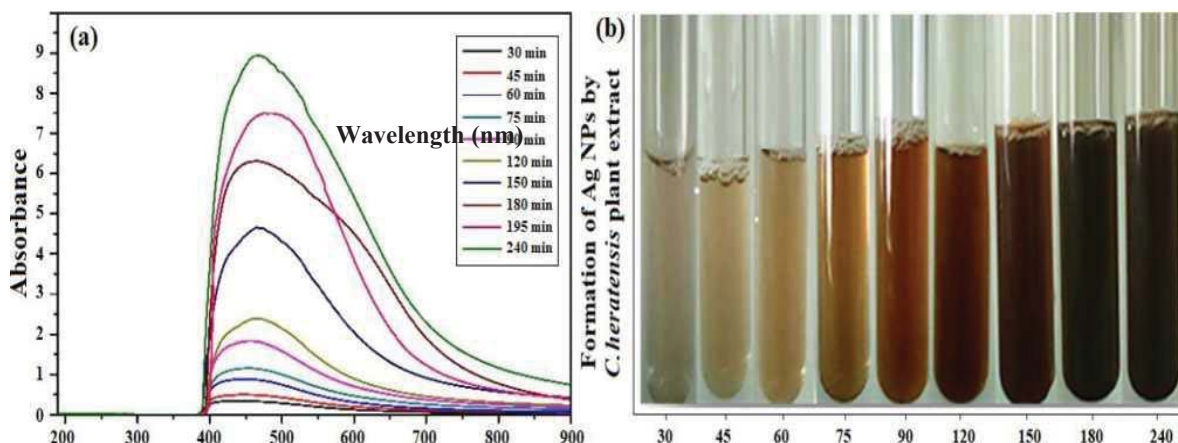


**Fig. 3.** (a) UV-Vis spectra of Ag NPs as a function of interaction time using 0.025 M  $\text{Ag}^+$  and 1/20 extract at 100 °C, and (b) the corresponding optical images of silver NPs, as a function of reaction time.

**Effect of extract concentration.** Different concentrations (1/10, 1/20, 1/30, 1/40, 1/50) of the aqueous extract of *C. heratensis* were prepared by boiling of the aerial parts of plant (1.0 g) in 10, 20, 30, 40 and 50 ml of deionized water for 5 min. Then, the experiment was performed with addition of  $\text{AgNO}_3$  (0.025 M) solution with 1:1 mixing ratio at 100 °C for 4 h. Figure 4a shows the UV-Vis spectra of the NPs obtained on the different concentrations of *C. heratensis* extract. The results demonstrated that 1/20 extract concentration give the highest possible intensity for SPR band related to Ag NPs. With an enhancement in



concentration of the plant extract from 1/50 to 1/20, the SPR peak intensity increases. A red shift for the SPR band was appeared in 1/10 extract concentration exhibiting larger size nanoparticles in higher extract concentrations (Fig. 4a).

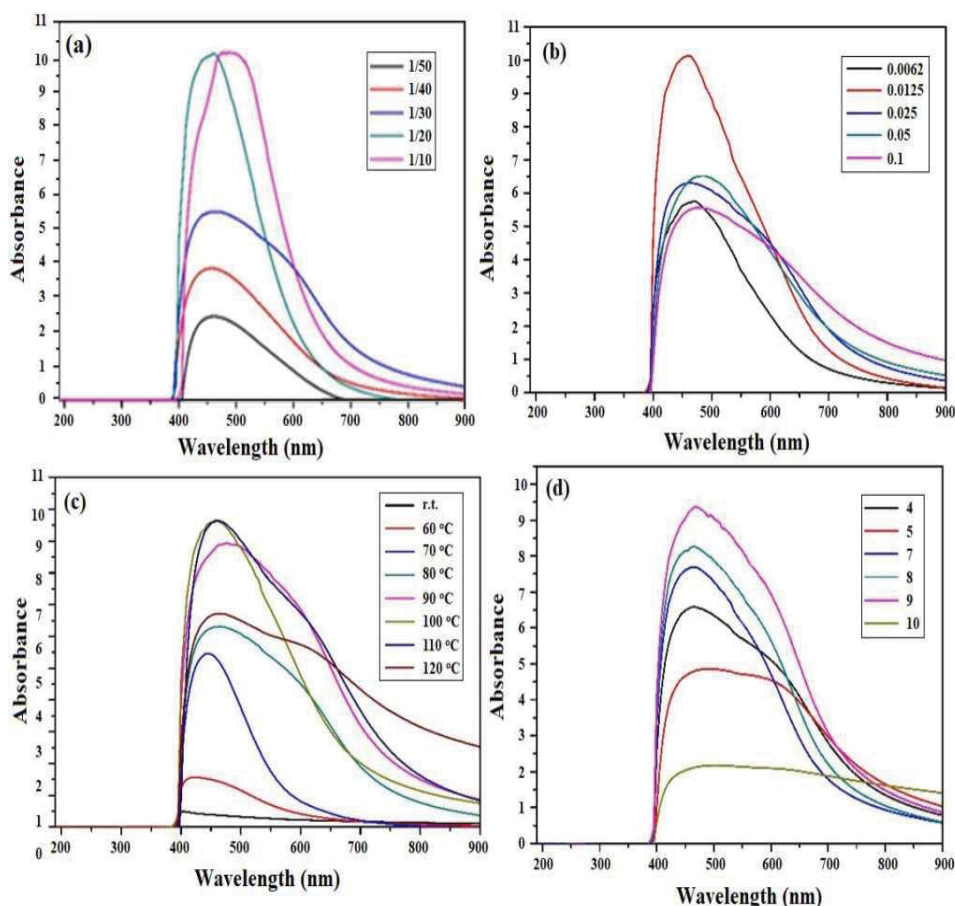


**Fig. 4.** UV-Vis spectra obtained from *C. heratensis* -mediated preparation of Ag NPs at: (a) plant extract concentration; (b) AgNO<sub>3</sub> concentration; (c) temperature; and (d) pH values of the reaction mixture

#### Effect of AgNO<sub>3</sub> concentration on Ag NPs synthesis.

The preparation of Ag NPs using *C. heratensis* extract (1/20) was investigated at different concentrations of AgNO<sub>3</sub> (0.0062, 0.0125, 0.025, 0.05, 0.1 M) under the same reaction conditions mentioned previously (Fig. 4b). According to the UV-Vis spectra obtained at various AgNO<sub>3</sub> concentrations, 0.0125 M AgNO<sub>3</sub> give the highest intensity of SPR band at 470 nm (Fig. 4b). No shift was observed in the peak position of SPR band with varying AgNO<sub>3</sub> concentration.

**Effect of temperature on Ag NPs synthesis.** The effect of temperature on the bio-synthesis of silver NPs is shown in Fig. 4c. The results displayed that temperature is an effective parameter for the bio-synthesis of NPs using *C. heratensis* extract. As shown in Fig. 4c, increase of temperature, increases the SPR absorption band, and the highest intensity was observed for SPR band at 100 °C. The intensity of SPR band shifts to lower wavelengths at higher temperatures from 100 °C. It reveals that the optimized temperature for the bio-synthesis of Ag NPs is 100 °C. A shoulder appeared in the visible region of UV-Vis spectra could be attributed to departure from spherical shape for a few NPs result in transverse plasmon vibrations in the Ag NPs [58].

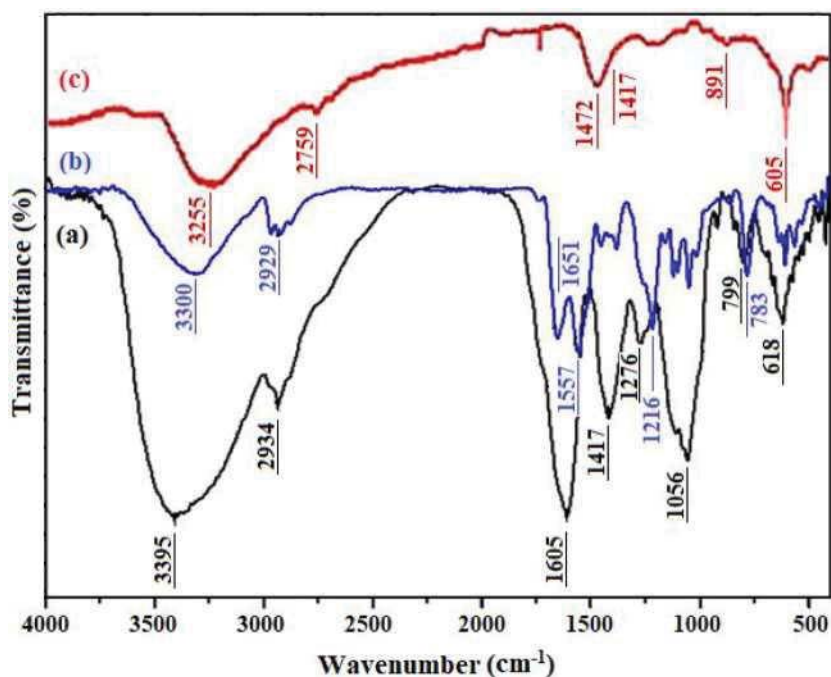


**Fig. 5.** FTIR spectra of (a) *C. heratensis* aqueous extract and the bio-synthesized, (b) Ag and (c) Fe<sub>3</sub>O<sub>4</sub> NPs using *C. heratensis* aqueous extract.

### Effect of pH

According to the literature, pH plays a vital role for the preparation of metal NPs [50,34]. To screen the effect of pH, the biosynthesis of Ag NPs was performed at various pHs as 4, 5, 7, 8, 9 and 10 using dilute acetic acid and sodium hydroxide solutions. Generally, the results illustrated that increasing the pH from 4-10 causes to increase in SPR band at  $X_{max} \sim 470$  nm, except pH 5 and 9. This behavior could be attributed to the increase of colloidal silver

nanoparticles and reduction rate [59]. It is well known that the particle size is expected to be larger in acidic medium than in basic, because, in basic medium, hydroxide ions charging the surface of NPs and thus maximum electrostatic/electrosteric repulsion occurs leading to decrease in agglomeration [60,61]. Moreover, at higher pHs than 9, species such as bioorganic-Ag (OH)<sub>x</sub> complex and AgOH/Ag<sub>2</sub>O colloid could be formed on the surface of particles [62]. It was found that the pH = 9 is ideal for the bio-synthesis of Ag NPs by *C. heratensis* extract. Furthermore, the observed single absorption band proposed that the prepared particles are nearly spherical in shape; because deviation from spherical shape provides another excess absorption band in the UV-Vis spectra in high pH values [60].

### Characterization of Nanoparticles

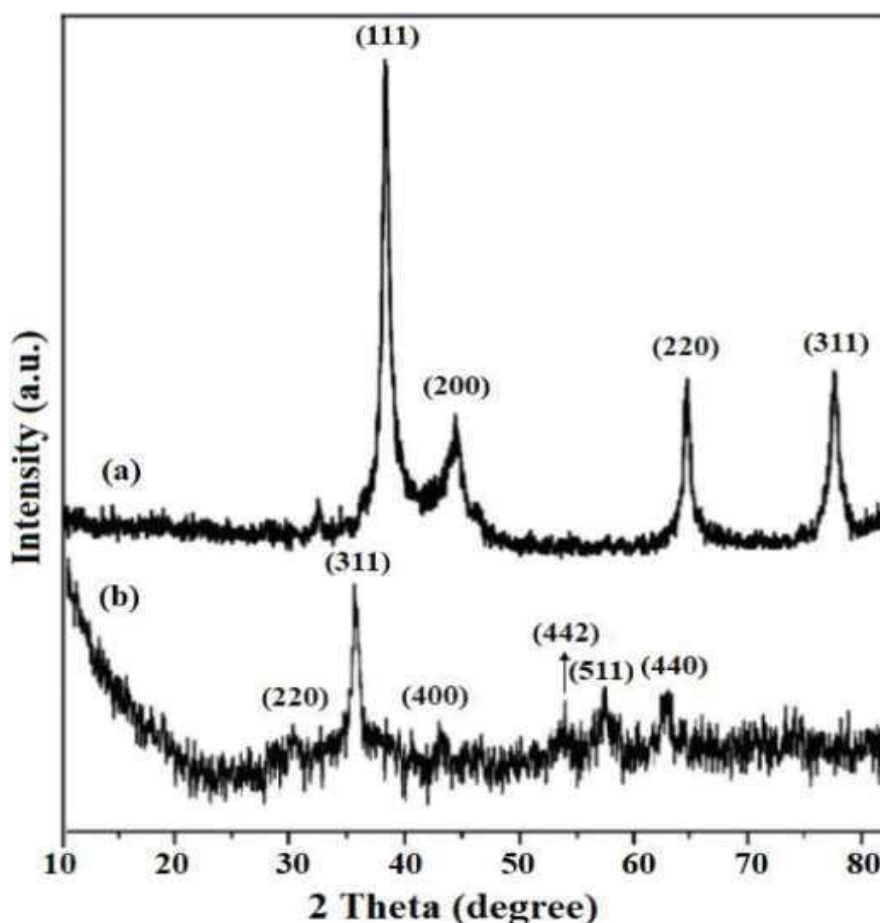


**Fig. 6.** XRD patterns of the bio-synthesized (a) Ag NPs, and (b) Fe<sub>3</sub>O<sub>4</sub> NPs using aqueous extract of *C. heratensis*



FTIR spectroscopy was applied to characterize and identify the functional groups of the bioactive components. FTIR spectrum of the plant extract (Fig. 5a) represent various functional groups related to the present biomolecules in the extract. The broad absorption band at  $3395\text{ cm}^{-1}$  and  $1056\text{ cm}^{-1}$  are may be due to O-H stretching and C-O stretching vibrations of different phenolic/alcoholic compounds; which are typical for polysaccharides [53]. The bands appeared at  $2934\text{ cm}^{-1}$  and  $1605\text{-}1417\text{ cm}^{-1}$  show stretching vibrations of aliphatic C-H and aromatic C=C bands, respectively. Also, a strong band at  $1276\text{ cm}^{-1}$  could be assigned to C-N band of amines. These molecules are responsible for the possible interactions between Ag and Fe<sub>3</sub>O<sub>4</sub> nanoparticles and the bioactive molecules that could be efficiently bind to metal as well as the reduction of Ag(0) and Fe ions [63], and subsequently bio-synthesis of nanoparticles. Accordingly, the biomolecules play a role of capping, stabilization and reduction for NPs leading to delayed aggregation and stabilization of silver nanoparticles [64]

The bio-synthesized Ag and Fe<sub>3</sub>O<sub>4</sub> NPs using *Cleome heratensis* plant extract were also studied by FTIR analysis and their corresponding spectra are shown in Fig. 5. The comparison of FTIR spectrum between the extract and Ag NPs showed only minor shifts in the position of the absorption bands. This indicates that silver NPs synthesized using the *C. heratensis* extract are successfully capped by functional groups of amides, alcohols, ketones and phenolic compounds on the silver particles involved in their reduction and stabilization. Moreover, decrease in intensity of the band around at  $3300\text{ cm}^{-1}$  implies the involvement of the hydroxyl group in the reduction process of nanoparticles (Fig. 5b).

The shift of wavenumbers also could be seen for the biosynthesis of Fe<sub>3</sub>O<sub>4</sub> NPs, confirming the interaction of bioactive molecules with Fe<sup>2+</sup> [65]. Also, a new absorption band at  $570\text{ cm}^{-1}$  is attributed to the newly formed Fe-O band of Fe<sub>3</sub>O<sub>4</sub> NPs [30].

The crystalline nature of the bio-synthesized nanoparticles was studied by XRD analysis. XRD pattern of the bio-synthesized Ag NPs showed face-centered cubic (FCC) structure (Fig. 6a). Four intense peaks at  $2\theta = 38.17^\circ$ ,  $44.17^\circ$ ,  $63.52^\circ$  and  $78.32^\circ$  correspond to the indices (111), (200), (220) and (311), respectively, completely in agreement with the facets of FCC structure of Ag NPs [66] and the reported standard of Joint Committee on Powder

Diffraction Standards (JCPDS) file No. 84-0713 [67]. The crystal structure of Fe<sub>3</sub>O<sub>4</sub> NPs synthesized by *C. heratensis* extract was also confirmed by their X-ray diffraction pattern. As shown in Fig. 6, there are six diffraction peaks with 2θ values of 30.55°, 35.83°, 43.40°, 54.07°, 57.34°, 63.04°, 74.44° corresponding to the crystal phases of (220), (311), (400), (442), (511) and (440), respectively. The results were completely in agreement with XRD standard of magnetite Fe<sub>3</sub>O<sub>4</sub> NPs with inverse cubic spinel phase [68] of the JCPDS No. 19-0629.

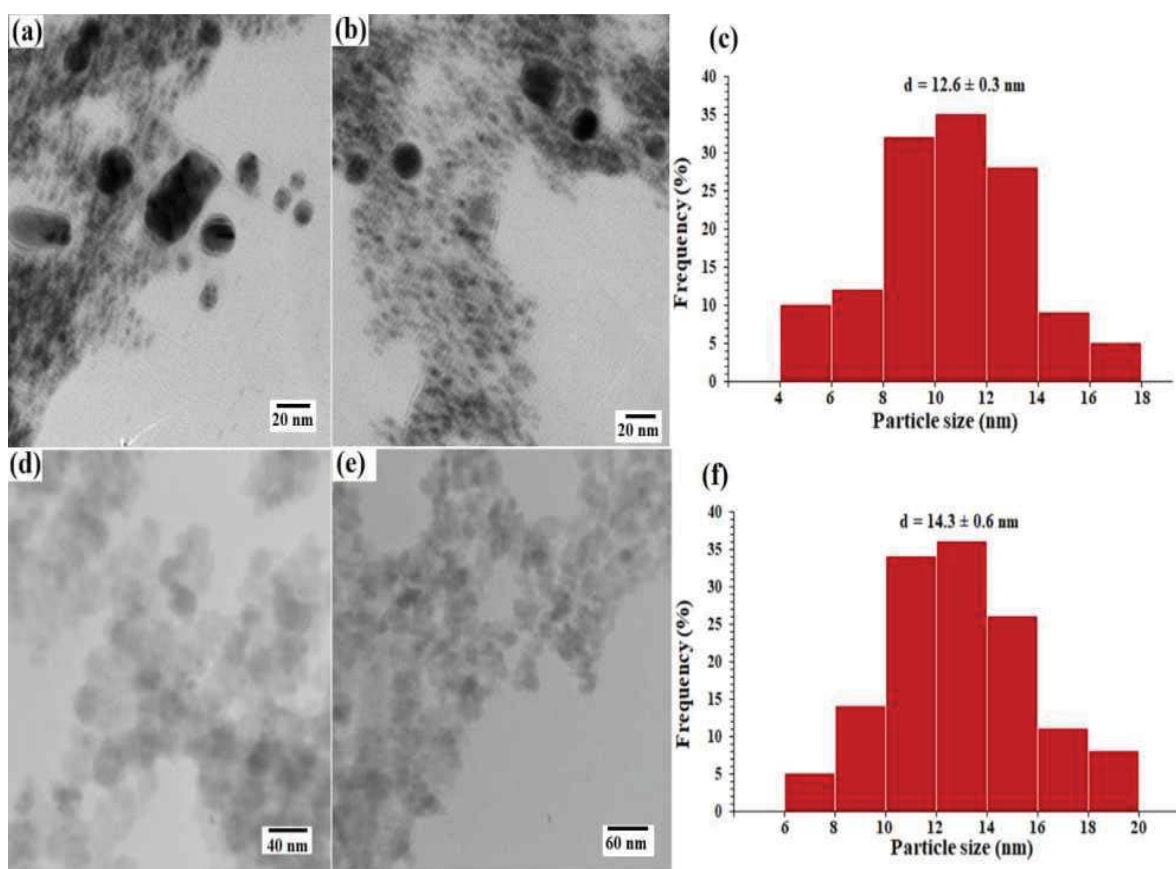


**Fig. 7.** TEM images and particles size distribution histogram of the bio-synthesized (a), (b), (c) Ag NPs and (d), (e), (f) Fe<sub>3</sub>O<sub>4</sub> NPs using aqueous extract of *C. heratensis*

The average size of the nanoparticles was measured by the most intensity XRD peak for each XRD pattern of nanoparticles using Scherer's equation:  $d = 0.9 \lambda / \Delta 2\theta \cos \theta$ ; where  $d$  is the average particle size,  $\lambda$  is the wavelength of Cu-K $\alpha$  irradiation (0.1541 nm),  $\Delta 2\theta$  is the full width at half maximum intensity of the diffraction peak, and  $\theta$  is diffraction angle for the

most intensity peak. The size of the nanoparticles was found 12.27 nm for silver NPs and 14.13 nm for Fe<sub>3</sub>O<sub>4</sub> NPs.

TEM micrographs and particles size distribution for the nanoparticles are shown in Fig. 7. TEM images of Ag and Fe<sub>3</sub>O<sub>4</sub> NPs revealed the spherical shape of the nanoparticles with an average size of 12 nm and 14 nm for the biosynthesized Ag and Fe<sub>3</sub>O<sub>4</sub> NPs, respectively. These results support the size obtained by Scherer's equation. Also, the nanoparticles demonstrate a narrow size distribution (Figs. 7c and f). Figures 7c and d demonstrate that the particle size of Ag and Fe<sub>3</sub>O<sub>4</sub> nanoparticles mostly ranges between 8-14 and 10-16 nm, respectively.

Magnetization behavior of the biosynthesized Fe<sub>3</sub>O<sub>4</sub> NPs is shown in Fig. 8a. As can be seen in Fig. 8a, VSM analysis gives the magnetization saturation values for Fe<sub>3</sub>O<sub>4</sub> of 70 emu g<sup>-1</sup> without any hysteresis; that is an intrinsic property of superparamagnetic nanoparticles [65]. Also, the magnetization and demagnetization curves are coincident and both coercivity and remanent magnetization are equal to zero. As shown in Fig. 8, the biosynthesized Fe<sub>3</sub>O<sub>4</sub> NPs with 70 amu g<sup>-1</sup> saturation magnetization value is comparable with those prepared by traditional co-precipitation method, indicating the potential of the present method for the preparation of various magnetic and non-magnetic nanoparticles.

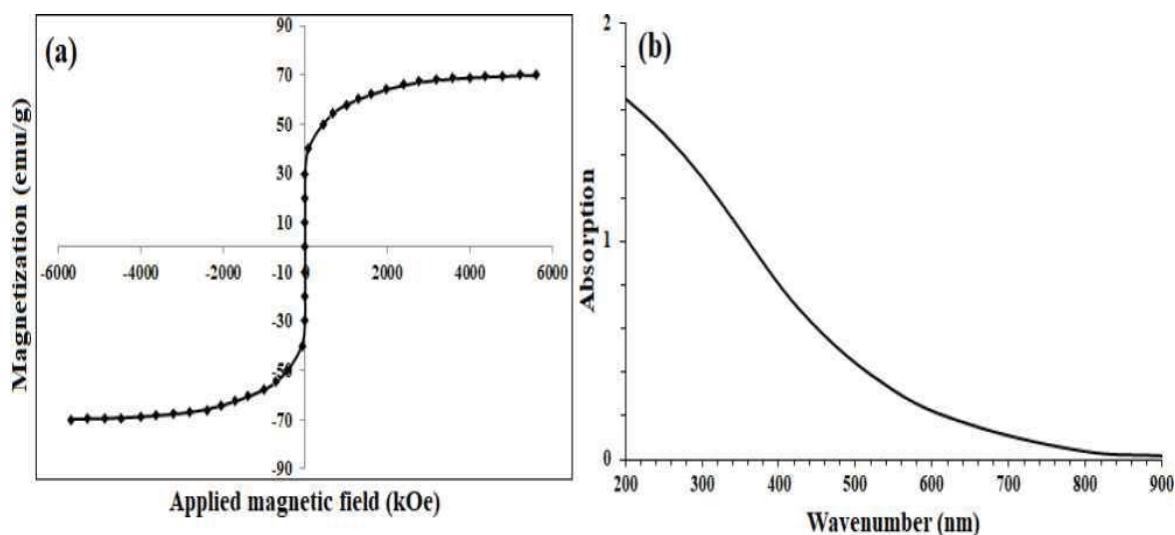


Fig. 8. (a) Magnetization curve, and (b) UV-Vis spectra of the bio-synthesized Fe<sub>3</sub>O<sub>4</sub> NPs using *C. heratensis* plant extract.



UV-Vis spectrum of the bio-synthesized Fe<sub>3</sub>O<sub>4</sub> NPs shows a continuous absorption in the range of 200-800 nm. The results are compatible with the reported UV-Vis spectra for the bio-synthesized Fe<sub>3</sub>O<sub>4</sub> using plant extracts [69,70]. The color of the reaction mixture iron salts changed from light brown to black verifying the formation of Fe<sub>3</sub>O<sub>4</sub> NPs in the mixture [69].

## CONCLUSIONS

In this research, we have developed facile bio-synthesis of iron oxide and silver NPs using aqueous extract of *C. heratensis* plant as a reducing and stabilized agent. Crystal structure of the NPs were confirmed by XRD as well as FTIR analyses. The size of the silver and Fe<sub>3</sub>O<sub>4</sub> NPs were found to be 12.27, 14.12 nm respectively, completely in agreement with the size obtained from Scherer's equation with the result of XRD analysis. VSM analysis exhibited a magnetization saturation value of 70 emu g<sup>-1</sup> for Fe<sub>3</sub>O<sub>4</sub> NPs. Investigation on reaction parameters revealed that the maximum efficiency is achieved for nanoparticles in the following conditions: 4 h, 100 °C, pH 9, extract concentration of 1/20 g ml<sup>-1</sup> and concentration of silver nitrate 0.0125 molar with 1:1 mixing ratio. The active biomolecules existing in the plant were responsible for the quick reduction of silver and iron ions to the corresponding metallic nanoparticles. Economic, non-toxic, using cheap and accessible materials, being environmentally benign and clean, versatility, and absence of any surfactant or toxic reagents are some of the advantages of the present work for the preparation of metallic nanoparticles. The present method proposed an ecofriendly suitable alternative to the available traditional and chemical methods.

## Disclosure Statement

No potential conflict of interest was reported by the authors.

## ACKNOWLEDGEMENTS

The authors are thankful to Research Council of University of Birjand for providing all the necessary facilities to carry out the research work.



## REFERENCES

- [1] S.K. Sahoo, S. Parveen, J.J. Panda, *Nanomedicine* 3 (2007) 20.
- [2] V. Bhalla, H. Tyagi, *Renew. Sust. Energ. Rev.* 84 (2018) 12.
- [3] S. Ahmed, M. Ahmad, B.L. Swami, S. Ikram, *J. Adv. Res.* 7 (2016) 17.
- [4] M.A. Albrecht, C.W. Evans, C.L. Raston, *Green Chem.* 8 (2006) 417.
- [5] C.B. Ong, L.Y. Ng, A.W. Mohammad, *Renew. Sust. Energ. Rev.* 81 (2018) 536.
- [6] V.K. Sharma, R.A. Yngard, Y. Lin, *Adv. Colloid Interface Sci.* 145 (2009) 83.
- [7] Q. Chaudhry, L. Castle, *Trends Food Sci. Technol.* 22(2011) 595.
- [8] M.A. Smith, M. Dauk, H. Ramadan, H. Yang, L.E. Seamons, R.P. Haslam, F. Beaudoin, I. Ramirez- Erosa, L. Forseille, *Plant Physiol.* 161 (2013) 81.
- [9] K. Chaloupka, Y. Malam, A.M. Seifalian, *Trends Biotechnol.* 28 (2010) 580.
- [10] T.W. Prow, J.E. Grice, L.L. Lin, R. Faye, M. Butler, W. Becker, E.M. Wurm, C. Yoong, T.A. Robertson, H.P. Soyer, M.S. Roberts, *Adv. Drug Deliv. Rev.* 63 (2011) 470.
- [11] P.J. Rivero, E. Ibanez, J. Goicoechea, A. Urrutia, I.R. Matias, F.J. Arregui, *Sens. Actuators B Chem.* 251 (2017) 624.
- [12] Hernandez-Arteaga, J.D.J.Z. Nava, E.S. Kolosovas-Machuca, J.J. Velazquez-Salazar, E. Vinogradova, M. Jose-Yacaman, H.R. Navarro- Contreras, *Nano Res.* 10 (2017) 3662.
- [13] P.R. Chang, J. Yu, X. Ma, D.P. Anderson, *Carbohydr. Polym.* 83 (2011) 640.
- [14] Tripathy, A.M. Raichur, N. Chandrasekaran, T.C. Prathna, A. Mukherjee, *J. Nanopart. Res.* 12 (2010) 237.
- [15] W. Weiss, W. Ranke, *Prog. Surf. Sci.* 70 (2002) 1.
- [16] D. Speliotis, *J. Magn. Mater.* 193 (1999) 29.
- [17] Karimzadeh, M. Aghazadeh, M.R. Ganjali, P. Norouzi, T. Doroudi, P.H. Kolivand, *Mater. Lett.* 189 (2017) 290.
- [18] O.K. Arriortua, M. Insausti, L. Lezama, I.G. de Muro, E. Garaio, J.M. de la Fuente, R.M. Fratila, M.P. Morales, R. Costa, M. Eceiza, M. Sagartzazu- Aizpurua, *Colloids Surf. B Biointerfaces.* 165 (2018) 315.
- [19] J.N. Solanki, Z.V.P. Murthy, *Colloids Surf. A Physicochem. Eng. Asp.* 359 (2010)





- [20] X. Hu, J.C. Yu, J. Gong, Q. Li, G. Li, *Adv. Mater.* 19 (2007) 2324.
- [21] V. Kumar, S.K. Yadav, *J. Chem. Technol. Biotechnol.* 84 (2009) 151.
- [22] J.P. Chen, L.L. Lim, *Chemosphere* 49 (2002) 363.
- [23] J. Li, Y. Wu, M. Yang, Y. Yuan, W. Yin, Q. Peng, Y. Li, X. He, *J. Am. Ceram. Soc.* 100 (2017) 5460
- [24] D.L. Paiva, A. LAndrade, M.C. Pereira, J.D. Fabris, R.Z. Domingues, M.E. Alvarenga, *Hyperfine Interact.* 232 (2015) 19.
- [25] B.M. Kumfer, K. Shinoda, B. Jeyadevan, I.M. Kennedy, *J. Aerosol Sci.* 41 (2010) 257.
- [26] L. Zhang, Q. Fan, X. Sha, P. Zhong, J. Zhang, Y. Yin, C. Gao, *Chem. Sci.* 8 (2017) 6103.
- [27] G.S. Ghodake, N.G. Deshpande, Y.P. Lee, E.S. Jin, *Colloids Surf. B Biointerfaces* 75 (2010) 584.
- [28] R. Sanghi, P. Verma, *Bioresour. Technol.* 100 (2009) 501.
- [29] Ronavari, D. Kovacs, N. Igaz, C. Vagvolgyi, I.M. Boros, Z. Konya, I. Pfeiffer, M. Kiricsi, *Int. J. Nanomedicine* 12 (2017) 871.
- [30] Singhal, N. Singhal, A. Bhattacharya, A. Gupta, *Inorg. Nano-Met. Chem.* 47 (2017) 1520.
- [31] Tripathy, A.M. Raichur, N. Chandrasekaran, T.C. Prathna, A. Mukherjee, *J. Nanopart. Res.* 12 (2010) 237.
- [32] V. Kumar, S.C. Yadav, S.K. Yadav, *J. Chem. Technol. Biotechnol.* 85 (2010) 1301.
- [33] Saxena, R.M. Tripathi, F. Zafar, P. Singh, *Mater. Lett.* 67 (2012) 91.
- [34] S.P. Chandran, M. Chaudhary, R. Pasricha, A. Ahmad, M. Sastry, *Biotechnol. Prog.* 22 (2006) 577.
- [35] O.A. Ojo, B.E. Oyinloye, A.B. Ojo, O.B. Afolabi, O.A. Peters, O. Olaiya, A. Fadaka, J. Jonathan, O. Osunlana, *J. Bionanosci.* 11 (2017) 292.
- [36] J.U. Chandirika, G. Annadurai, *Global J. Biotechnol. Biochem.* 13 (2018) 07.
- [37] S.S. Shankar, A. Rai, A. Ahmad, M. Sastry, *J. Colloid Interface Sci.* 275 (2004) 496.
- [38] S. Francis, S. Joseph, E.P. Koshy, B. Mathew, *Environ. Sci. Pollut. Res. Int.* 24



- (2017) 17347.
- [39] N. Ahmad, S. Sharma, M.K. Alam, V.N. Singh, S.F. Shamsi, B.R. Mehta, A. Fatma, Colloids Surf. B Biointerfaces 81 (2010) 81.
- [40] U.K. Sur, B. Ankamwar, S. Karmakar, A. Halder, P. Das, Mater. Today 5 (2018) 2321.
- [41] R. Brause, H. Moeltgen, K. Kleinermanns, Appl. Phys. B 75 (2002) 711.
- [42] J.M. Khaled, N.S. Alharbi, S. Kadaikunnan, A.S. Alobaidi, M.N. Al-Anbr, K. Gopinath, A. Aurmugam, M. Govindarajan, G. Benelli, J. Cluster Sci. 28 (2017) 3009.
- [43] K. Venugopal, H.A. Rather, K. Rajagopal, M.P. Shanthi, K. Sheriff, M. Illiyas, R.A. Rather, E. Manikandan, S. Uvarajan, M. Bhaskar, M. Maaza, J. [57] Photochem. Photobiol. B Biol. 167 (2017) 282.
- [44] S.G. Balwe, V.V. Shinde, A.A. Rokade, S.S. Park, [58] Y.T. Jeong, Catal. Commun. 99 (2017) 121.
- [45] Khodadadi, M. Bordbar, A. Yeganeh-Faal, M. [59] Nasrollahzadeh, J. Alloys Compd. 719 (2017) 82.
- [46] S. Raja, V. Ramesh, V. Thivaharan, Arab. J. Chem. 10 (2017) 253.
- [47] M.A. Nasser, S. Behraves, A. Allahresani, Iran. Chem. Commun. 5 (2017) 364.
- [48] S.M. Ghaderian, A.J.M. Baker, J. Geochem. Explor. [62] 92 (2007) 34.
- [49] S. Sungwarl, P. Supanee, J. Agric. Sci. 37 (2006) 232.
- [50] S. Somboon, S. Pimsamarn, Agric. Sci. J. 37 (2006) 232.
- [51] N. Jayaprakash, J.J. Vijaya, K. Kaviyarasu, K. Kombaiah, L.J. Kennedy, R.J. Ramalingam, M.A. Munusamy, H.A. Al-Lohedan, J. Photochem. Photobiol. B Biol. 169 (2017) 178.
- [52] S. Jokic, R. Sudar, S. Svilovic, S. Vidovic, M. Bilic, [66] D. Velic, V. Jurkovic, Czech J. Food Sci. 31 (2013) 116.
- [53] S.H. Yau, B.A. Ashenfelter, A. Desireddy, A.P. [67] Ashwell, O. Varnavski, G.C. Schatz, T.P. Bigioni, T.
- [54] Goodson, J. Phys. Chem. C 121 (2017) 1349.
- [55] M.A. Noginov, G. Zhu, M. Bahoura, J. Adegoke, C.E. Small, B.A. Ritzo, V.P.



- Drachev, V.M. Shalaev, Opt. Lett. 31 (2006) 3022.
- [56] K.G. Stamplecoskie, J.C. Scaiano, J. Am. Chem. Soc. 010) 1825.
- [57] J. Baharara, F. Namvar, T. Ramezani, N. Hosseini, R. Mohamad, Molecules 19 (2014) 4624.
- [58] Kaurinovic, M. Popovic, S. Vlaisavljevic, S. Trivic, Molecules 16 (2011) 7401.
- [59] C.R. Rao, D.C. Trivedi, Mater. Chem. Phys. 99 (2006) 354.
- [60] C.W. Haminiuk, G.M. Maciel, M.S. Plata-Oviedo, R.M. Peralta, Int. J. Food Sci. Technol. 47 (2012) 2023.
- [61] F.S. Hosseinian, T. Beta, J. Agric. Food Chem. 55 (2007) 10832.
- [62] R.L. Prior, X. Wu, Free Radical Res. 40 (2006) 1014.
- [63] M.M. Khalil, E.H. Ismail, K.Z. El-Baghdady, D. Mohamed, Arab. J. Chem. 7 (2014) 1131.
- [64] W. Wrotniak-Drzewiecka, S. Gaikwad, D. Laskowski, H. Dahm, J. Niedojadlo, A. Gade, M. Rai, Austin J. Biotechnol. Bioengin. 1 (2014) 7.
- [65] K. Jyoti, M. Baunthiyal, A. Singh, Austin J. Biotechnol. Bioeng. 9 (2016) 217.
- [66] S. Kanagasubbulakshmi, K. Kadirvelu, Defence Sci. J. 2 (2017) 422.
- [67] P. Prakash, P. Gnanaprakasam, R. Emmanuel, S. Arokiyaraj, M. Saravanan, Colloids Surf. B Biointerfaces 108 (2013) 255.
- [68] Son-di, B. Salopek-Son-di, J. Colloid Interface Sci. 275 (2004) 177.
- [69] Mahdavi, M.B. Ahmad, M.J. Haron, Y. Gharayebi, K. Shameli, B. Nadi, J. Inorg. Organomet. Polym. Mater. 23 (2013) 599.
- [70] Y.P. Yew, K. Shameli, M. Miyake, N. Kuwano, N.B.B.A. Khairudin, S.E.B. Mohamad, K.X. Lee, Nanoscale Res. Lett. 11 (2016) 276.
- [71] Basavegowda, K.B.S. Magar, K. Mishra, Y.R. Lee, New J. Chem. 38 (2014) 5415.